Brief Papers

CPG Network Optimization for a Biomimetic Robotic Fish via PSO

Junzhi Yu, *Senior Member, IEEE*, Zhengxing Wu, Ming Wang, and Min Tan

***Abstract*— In this brief, we investigate the parameter optimization issue of a central pattern generator (CPG) network governed forward and backward swimming for a fully untethered, multijoint biomimetic robotic fish. Considering that the CPG parameters are tightly linked to the propulsive performance of the robotic fish, we propose a method for determination of relatively optimized control parameters. Within the framework of evolutionary computation, we use a combination of dynamic model and particle swarm optimization (PSO) algorithm to seek the CPG characteristic parameters for an enhanced performance. The PSO-based optimization scheme is validated with extensive experiments conducted on the actual robotic fish. Noticeably, the optimized results are shown to be superior to previously reported forward and backward swimming speeds.**

***Index Terms*— Central pattern generator (CPG), neurodynamic systems, parameter optimization, robotic fish.**

I. Introduction

Biorobotics research has received increasing attention in recent years, where robots have been either applied to address specific biological questions or to improve the traditional mechatronic systems [1], [2]. Inspired by the speed, efficiency, and agility of biological fish, different types of fishlike robots termed robotic fish have been developed [3]–[6]. Instead of using propellers, a robotic fish usually achieves propulsion and maneuvers through movements of body and/or finlike appendages. Besides serving as a testbed for studying fish swimming, robotic fish holds great promise for a variety of underwater applications such as underwater exploration, patrol, aquatic monitoring, and mobile sensing. Despite their appeal, current robotic fish is still far inferior to their biological counterparts in terms of speed and maneuverability, demanding further research into swimming mechanisms and control methods.

Recently, central pattern generators (CPGs) are increasingly used to control the rhythmic movements such as legged walking, crawling, flying, and swimming in robotics [7], [8]. Biological CPGs are dedicated neural networks located in the spinal cord, which have the capability of producing coordinated patterns of rhythmic activity, such as respiration, chewing, or leg movement during walking. In particular, CPGs can produce rhythmic signals without any rhythmic inputs from sensory feedback or higher control centers. In addition, CPGs have strong robustness, good adaptability, and easily adjustable output signals. These fascinating features make CPGs suitable for locomotion control of robots with multiple joints or DOFs and even of hyperredundant robots [8].

As a specific application case, the CPG-based control is widely used to generate fishlike swimming for various robotic fish [9]–[11]. Compared with the traditional fish body wave fitting method, CPGs as online gait generators simply alter the characteristics of output signals and maintain smooth and continuous even if parameters are abruptly altered. Therefore, the CPGs are well suited to implement versatile swimming patterns such as forward swimming, backward swimming, and turning [12], [13]. Unfortunately, almost all CPGs involve several differential equations with many uncertain parameters, requiring the user to choose the values of parameters heuristically to achieve good performance. Moreover, relatively large number of optimization parameters indicating a multiobjective optimization should be properly tackled. In this sense, how to tune and modulate the CPG parameters to generate optimal patterns for robotic fish is still challenging. For instance, Wang *et al.* [14] proposed a method to determine the CPG parameters through discretizing the fish body equations. Jeong *et al.* [15] used particle swarm optimization (PSO) algorithm to seek CPG parameters so as to minimize the difference between the desired traveling wave and the link flapping wave forms of the robotic fish. Hu *et al.* [16] presented a learning method to attain the desired signals through designing the learning rules for intrinsic frequency, coupling weight, and amplitude of the CPGs. Niu *et al.* [17] presented a locomotion learning method for an anguilliform robotic fish based on CPGs through extracting the swimming pattern from a real fish. Although steady forward swimming governed by the artificial CPGs has been extensively investigated, the simultaneous optimization and comparison of both forward and backward swimming on the same robotic platform were rarely tackled.

This brief, on the basis of our previous work about the CPG-governed swimming modeling and control [18], [19], aims at offering a CPG network optimization method to directly maximize both forward and backward swimming speeds, rather than to optimize the traveling wave [15]. In particular, a relatively accurate dynamic model is first developed to guide the selection of control parameters and the search of suitable swimming patterns. Then, the standard PSO algorithm [20] with several chaos random disturbances is exploited to refine the feature parameters of the CPG network. Finally, the formed optimization schemes are extensively validated on the real robot. The specific contribution made, here, is that the integration of dynamic model and PSO algorithm fairly facilitates the CPG network optimization, thereby greatly enhancing both forward and backward swimming performance. Compared with the previous research on PSO-based CPG control [21], a hybrid use of dynamic model and PSO is proposed and a higher maximum swimming speed of over 1.15 BL/s (body length per second) is resulted. As opposed to the reported robotic fish whose maximum backward swimming speeds were around 0.092 BL/s [22] and 0.16 BL/s [23], the robot presented here with a top backward swimming speed of 0.51 BL/s is far superior, revealing that the backward swimming ability of robotic fish can be greatly capitalized on.

Manuscript received August 15, 2014; revised May 28, 2015; accepted July 19, 2015. Date of publication August 7, 2015; date of current version August 15, 2016. This work was supported in part by the National Natural Science Foundation of China under Grant 61375102 and Grant 61333016, in part by the Beijing Natural Science Foundation under Grant 3141002, in part by Project-Based Personnel Exchange Programme with CSC and DAAD (2013), and in part by the State Key Laboratory of Alternate Electrical Power System with Renewable Energy Sources under Grant LAPS16006. *(Corresponding author: Junzhi Yu.)*

J. Yu, Z. Wu, and M. Tan are with the State Key Laboratory of Management and Control for Complex Systems, Institute of Automation, Chinese Academy of Sciences, Beijing 100190, China (e-mail: junzhi.yu@ia.ac.cn; zhengxing.wu@ia.ac.cn; min.tan@ia.ac.cn).

M. Wang is with the School of Information and Electrical Engineering, Shandong Jianzhu University, Jinan 250101, China (e-mail: xclwm@sdjzu.edu.cn).

Color versions of one or more of the figures in this paper are available online at http://ieeexplore.ieee.org.

Digital Object Identifier 10.1109/TNNLS.2015.2459913

2162-237X © 2015 IEEE. Personal use is permitted, but republication/redistribution requires IEEE permission.
See http://www.ieee.org/publications_standards/publications/rights/index.html for more information.

The remainder of this brief is organized as follows. We start by offering an overview of the dynamic modeling and the CPG-based locomotion control for the robotic fish in Section II. We then proceed to develop the PSO-based parameter optimization method for the CPG network in Section III. Testing results and discussion are provided in Section IV. Finally, Section V gives some concluding remarks.

II. Dynamic Modeling and Locomotion Control

A. Dynamic Modeling of Robotic Fish

Most fish generate thrust by undulating their bodies or caudal fins to transfer momentum to the surrounding water. In particular, the fish bend their bodies into a backward traveling wave which extends from the nose to the caudal fin with varying amplitude along the traveling path. In this context, many approaches and ideas have been developed to replicate fishlike swimming. For the sake of simplicity, a robotic fish can be considered as a three-part propulsion system, i.e., a stiff anterior body, a flexible posterior body, and an oscillating lunate caudal fin. In particular, the well-streamlined rigid anterior body is passively sideslipped to some extent, while the flexible posterior body composed of many segments (or links) takes on lateral oscillating movements. The most widely used kinematic model of fish swimming is Lighthill's fish body-wave equation [24]

$$Y_{\text{body}}(X,t) = (c_1 X + c_2 X^2)\sin(kX + \Omega t) \tag{1}$$

where Y_{body} denotes the transverse displacement along the lateral direction of the fish body, X indicates the displacement along the main axis, c_1 and c_2 are applied to adjust the specific amplitude envelope of the entire fish body, which can be obtained from the behaviors of real fish; k represents the body wave number ($k = 2\pi/\lambda$), λ is the body wave length, and Ω decides the body wave frequency.

Without loss of generality, suppose that the robotic fish has n links including the stiff anterior part (the 0th link) and the caudal fin (the $n-1$th link). Based on the generalized active forces and generalized inertia forces on this n-link mechanism, we can obtain the dynamic equations using the Kane's method. Please refer to [18] for more details

$$K_{\text{inr}} + K_{\text{Ar}} + Q_r = 0 \quad (r = 0, \ldots, n+2) \tag{2}$$

where K_{inr} denotes the generalized inertia forces of the propulsion system, K_{Ar} indicates the generalized inertia forces due to the added mass for the entire system, and Q_r stands for the generalized active forces.

Once the kinematics of the robotic fish is determined, we can numerically evaluate its dynamic performance by solving the well-configured dynamic equations (2). That is, simulation results including the velocities in the X- and Y-axes, the angular velocity of the fish head, as well as corresponding trajectories can be yielded. However, it is intractable to construct an accurate dynamic model of fishlike swimming owing to complicated, nonlinear, and unsteady flow characteristics [25]. We remark that this brief is not an attempt to control fishlike swimming in a dynamic model manner, but in a bioinspired CPG model manner.

B. CPG-Based Locomotion Control

To achieve flexible fishlike locomotion, a heuristic approach is to mimic swimming kinematics (1) through fish body wave fitting. However, this body wave-based swimming control should be appropriately discretized and parameterized for a specific swimming pattern. Furthermore, the swimming stability of a desired pattern and the smooth transition between two different patterns are hardly guaranteed, particularly when a perturbation occurs unexpectedly in the course of a movement. Therefore, other alternatives should be sought to ensure stability and smoothness of fishlike swimming. Inspired by the lamprey, an eellike fish whose propulsion is governed by activity in its spinal neural network, some CPG-based models have been proposed to generate fishlike swimming [8]. As an online gait generator, the CPG network certainly possesses several appealing properties for the control of locomotion in robotic fish. For instance, CPGs typically generate smooth modulations of multimodal locomotion even when the control parameters are suddenly changed. Meanwhile, CPGs have outstanding quality of distributed control, especially for the robotic fish with many oscillating links [7].

Before building an artificial CPG controller, a suitable CPG control model should be decided. In this brief, Hopf oscillator, which is commonly used as the dynamic model of engineered CPGs, is adopted. A prominent merit is its limit cycle which is stable against small perturbations, together with the intrinsic synchronization property. Besides, there are explicit parameters related to the oscillator's frequency and amplitude, which are important characteristics to determine the swimming performance of a robotic fish. Therefore, we can shape the output through modulating corresponding parameters with ease. The dynamics of the Hopf oscillator is described by the following differential equations:

$$\begin{cases} \dot{x} = -\omega y + x(m - x^2 - y^2) \\ \dot{y} = \omega x + y(m - x^2 - y^2) \end{cases} \tag{3}$$

where x and y denote the state variables of the oscillator. ω and m stand for the intrinsic oscillation frequency and amplitude, respectively.

As a general rule, the phase is crucial to understand synchronization behavior. The sensitivity of the phase on perturbations can be analyzed by examining the form of the limit cycle. Within this framework, a method to predict phase relationships between coupled phase oscillators is formulated by introducing a coupling matrix (Q) and a rotation matrix (R) [26]. Following this idea, we add a perturbation term (P_i) to our CPG model:

$$\begin{aligned} P_i &= h_1 Q_1 R_1 \begin{bmatrix} x_{i-1} \\ y_{i-1} \end{bmatrix} + h_2 Q_2 R_2 \begin{bmatrix} x_{i+1} \\ y_{i+1} \end{bmatrix} \\ &= \begin{bmatrix} h_1 x_{i-1}\cos\varphi_i + h_1 y_{i-1}\sin\varphi_i \\ h_2 x_{i+1}\sin\varphi_{i+1} + h_2 y_{i+1}\cos\varphi_{i+1} \end{bmatrix} \end{aligned} \tag{4}$$

where h_1 and h_2 are coupling weights that regulate the speed of convergence, Q_1 and Q_2 are the coupling matrices, R_1 and R_2 are the rotation matrices, φ_i means the phase difference between the $i-1$th and ith oscillators, and here

$$\begin{aligned} Q_1 &= \begin{bmatrix} 1 & 0 \\ 0 & 0 \end{bmatrix}; \quad R_1 = \begin{bmatrix} \cos\varphi_i & \sin\varphi_i \\ -\sin\varphi_i & \cos\varphi_i \end{bmatrix} \\ Q_2 &= \begin{bmatrix} 0 & 0 \\ 0 & 1 \end{bmatrix}; \quad R_2 = \begin{bmatrix} \cos\varphi_{i+1} & -\sin\varphi_{i+1} \\ \sin\varphi_{i+1} & \cos\varphi_{i+1} \end{bmatrix}. \end{aligned} \tag{5}$$

Furthermore, considering that rotational maneuvers of real fish result from asymmetrical kinematics, we incorporate a directional bias b_i into the differential equations to induce asymmetrical maneuvers. It should be noted that b_i can be regarded as an on-demand feedback signal related to the ith oscillator in swimming orientation modulation. As a result, a modified CPG model comprising a set of hybrid Hopf oscillators is obtained, in which the phase differences between the oscillators can be arbitrarily chosen according to the

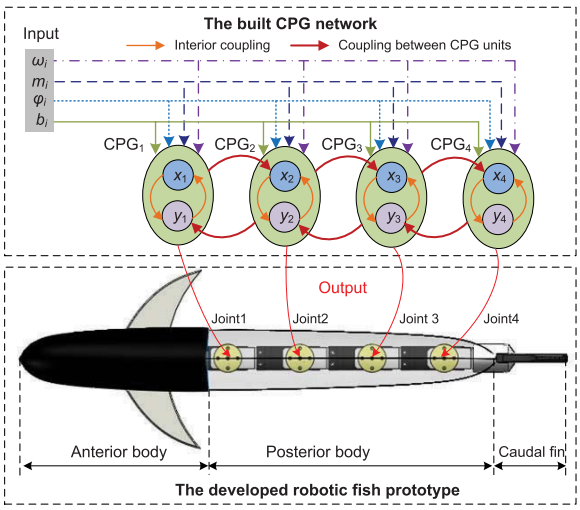

(a)

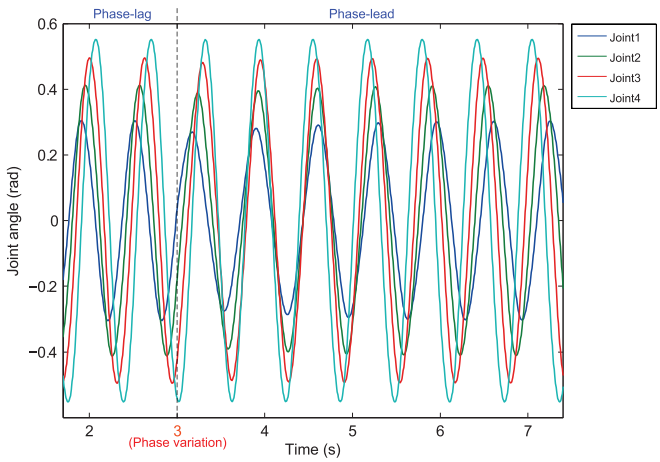

(b)

Fig. 1. CPG network for generating fishlike swimming. (a) Topology of the built CPG network. (b) CPGs activity during transition from forward to backward swimming.

requirements of the locomotion control

$$\begin{cases} \dot{x}_i = -\omega_i(y_i - b_i) + x_i\left(m_i - x_i^2 - (y_i - b_i)^2\right) \\ \qquad + h_1(x_{i-1}\cos\varphi_i + (y_{i-1} - b_{i-1})\sin\varphi_i) \\ \dot{y}_i = \omega_i x_i + (y_i - b_i)\left(m_i - x_i^2 - (y_i - b_i)^2\right) \\ \qquad + h_2(x_{i+1}\sin\varphi_{i+1} + (y_{i+1} - b_{i+1})\cos\varphi_{i+1}) \\ z_i = d_i y_i \end{cases} \tag{6}$$

where x_i and y_i indicate the state variables of the ith oscillating neurons. ω_i and m_i denote the intrinsic oscillation frequency and amplitude. φ_i stands for the phase difference between the $i-1$th and ith oscillators. b_i is the directional bias for state variable y_i. h_1 and h_2 stand for the coupling strengths. z_i and d_i indicate the output signal of the ith CPG and the amplification coefficient, respectively. In this brief, $b_i = 0$ holds since only steady swimming is considered. Meanwhile, the same frequency parameter $\omega_i = \omega$ and phase relationship parameter $\varphi_i = \varphi$ are used for all oscillators.

After the CPG control model is chosen, the following task is to determine the coupling relationship and topology of the network. As shown in Fig. 1(a), a possible network topology illustrating coupled connections of the CPGs is constructed, which coincides with the propulsion configuration of the robotic fish. Within this network, the CPGs adopt a simple adjacent coupling for relatively less parameters. Each CPG unit individually governs an oscillating body joint. Therefore, we can separately adjust the oscillatory amplitude of each joint for better performance. By contrast, a constant oscillatory amplitude often holds in the fish body wave method, which is basically constrained by the envelope parameters c_1 and c_2.

In addition, many anguilliform swimmers like lampreys are able to perform both forward and backward swimming by altering the propagation direction of the propulsive wave, especially when in danger. Biologists suggest that backward swimming has a relationship with the excitability order between anterior and posterior body parts. However, simple reversing of the forward control law does not apply to a carangiform fish whose large-amplitude undulation is largely confined to the posterior third of its body. Thus, seeking an appropriate backward swimming pattern for the carangiform robotic fish is very difficult and demands in-depth kinematic analysis [23]. Because of the parameter φ in the built CPG network, we can easily change the phase relationship between the oscillating joints for backward swimming, making it possible to replicate the backward swimming relatively easily. An illustrative example of the robotic fish switching from forward to backward swimming with involved CPGs activity is given in Fig. 1(b). At $0 < t < 3$ s, the phase-lag control signals are utilized to generate a backward traveling wave for forward swimming. Then, the phase-lead control signals are exploited to activate backward swimming after $t = 3$ s. During this sudden discontinuous switch, as can be observed, the CPGs signals are continuous and smooth. It partially demonstrates the CPG-based control merit in realizing a smooth and effective transition between the desired gaits.

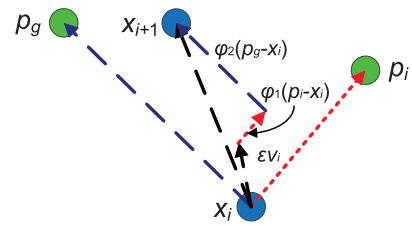

Fig. 2. Schematic of movement for the particle in the PSO.

III. Optimization of CPG Network via PSO

As is previously identified, the built CPG network has several characteristic parameters (e.g., amplitude, frequency, and phase lag) which are closely related to the propulsive performance. Naturally, a better locomotion performance is expected by a combined usage of the CPG network and effective optimization algorithms.

A. Particle Swarm Optimization

As a swarm intelligence-based algorithm, the PSO algorithm proposed by Kennedy and Eberhart in 1995 is inspired by social behaviors like flocks of birds or schools of fish [20]. In a D-dimensional space, there are m particles named $\mathbf{X} = (\mathbf{x}_1, \ldots, \mathbf{x}_m)$ in a swarm. Each particle i is a D-dimensional vector, which has its own position $\mathbf{x_i} = (x_{i1}, \ldots, x_{iD})^T$ and velocity $\mathbf{v_i} = (v_{i1}, \ldots, v_{iD})^T$. During the optimization process, as shown in Fig. 2, particles store their best positions $p_i = (p_{i1}, \ldots, p_{iD})^T$ and global best position $p_g = (p_{g1}, \ldots, p_{gD})^T$, and update their positions and velocities by

$$\begin{cases} \mathbf{v_i(t+1)} = \varepsilon\mathbf{v_i(t)} + \psi_1(\mathbf{p_i(t)} - \mathbf{x_i(t)}) + \psi_2(\mathbf{p_g(t)} - \mathbf{x_i(t)}) \\ \mathbf{x_i(t+1)} = \mathbf{x_i(t)} + \mathbf{v_i(t+1)} \end{cases} \tag{7}$$

where ψ_1 and ψ_2 are determined as rand$(0, c_1)$ and rand$(0, c_2)$, respectively, and c_1 and c_2 are accelerative constants, which impact the convergence speed of the PSO algorithm. ε is the inertia weight which controls the influence of the previous velocity on the new velocity. When ε gets a big value, the PSO has a better global search ability. Otherwise, it has a better local search ability. Here, ε adopts a linear decrease strategy for a better optimization [27]

$$\varepsilon = \varepsilon_{\max} - \frac{(\varepsilon_{\max} - \varepsilon_{\min})j}{n} \tag{8}$$

where $\varepsilon_{\max}$ and $\varepsilon_{\min}$ indicate the maximum and minimum values of ε; j and n denote the current and maximum iterations, respectively.

In the PSO, each particle can update its own position in accordance with its best position (corresponding to individual cognition) and global best position (corresponding to social cognition). This means that each particle has the ability to perceive both own and swarm's best position, and can adjust its action based on these information. Hence, the whole swarm reveals swarm intelligence. Since it is easy to realize, can save computational cost, and can improve the convergence speed, the PSO is widely used in various fields [28], [29].

To avoid the prematurity and diversity reduction of the PSO, chaos random disturbances to the current optimal results are also employed. Specially, several chaos random particles will be produced to test the best global particle in every generation. If the global particle is not the best one, the chaos particle will replace it.

B. Optimization of the Average Propulsive Speed

Optimization is one of the most important problems in engineering practice. For a robotic fish, the propulsive speed is an important performance indicator. In this brief, the maximum average propulsive speed (u) of a four-joint robotic fish in q oscillating periods is selected as the optimization objective. Since a set of CPG feature parameters including amplitude, frequency, and phase lag have a crucial effect on speed control of the robotic fish, a nonlinear optimization problem with multiple parameters can be defined. Namely, we try to search optimal feature parameter set $\{m_1, m_2, m_3, m_4, \omega, \varphi\}$ while keeping h_1, h_2, and c constant for maximizing average propulsive speed. Notice that there is an increasing tendency for oscillatory amplitude of carangiform swimmers. The same constraint is enforced on the robotic fish. Other parameter ranges are decided by considering the characteristics of the robotic prototype and movements of the biological counterpart. Consequently, the average propulsive speed optimization problem is formulated as follows:

$$\max \bar{u} = \frac{1}{qT}\int_0^{qT} u(t)dt. \tag{9}$$

Subject to

$$\begin{cases} \omega_{\min} \le \omega \le \omega_{\max} \\ m_{\min} \le m_1 < m_2 < m_3 < m_4 \le m_{\max} \\ \varphi_{\min} \le \varphi \le \varphi_{\max}. \end{cases} \tag{10}$$

IV. Results and Discussion

In order to evaluate the proposed optimization scheme, dynamic simulations are conducted using MATLAB while aquatic self-propelled tests are made in indoor swimming pool. After achieving good agreement between the model's prediction and the observed data, we perform the PSO-based CPG network optimization for both forward and backward swimming. In particular, all aquatic tests are conducted on a fully untethered, four-joint subcarangiform robotic fish whose dimension is 49.5 cm long, 5 cm wide, and 8 cm high.

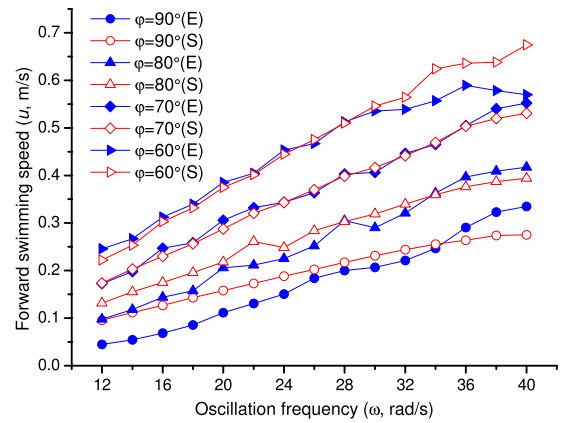

Fig. 3. Comparison of simulated and experimental forward swimming data under different oscillation frequencies. The used parameter values are $h_1 = 1.0$, $h_2 = 2.0$, $d_i = 5.0$, $m_1 = 5.0$, $m_2 = 15.0$, $m_3 = 35.0$, and $m_4 = 50.0$. Notice that S and E stand for simulated data and experimental data, respectively.

TABLE I
Optimization Range of CPG Parameters

Parameter	Range	Parameter	Range
m_1	$0 \sim 15$	m_2	$5 \sim 25$
m_3	$15 \sim 40$	m_4	$25 \sim 50$
ω	$0 \sim 30$	φ	$60° \sim 90°$

Each joint is actuated by a commercial-off-the-shelf servo, Hitec HS7940TH. The electronics is powered by a 7.4 V rechargeable lithium polymer battery pack. The whole robot weighs ~1.29 kg. The swimming performance of the robotic fish is evaluated by an additional vision measuring system. During testing, unless otherwise specified, the data points in subsequent figures were the averages of five runs.

A. Numerical Simulation and Experimental Results

First, we compared the model's prediction and the measured swimming data to verify the effectiveness of the built dynamic model. During experiments, different frequencies (ω) were varied over a large range of $\varphi_i \in [60°, 90°]$ with an increment of 10°. As can be observed from Fig. 3, the measured speed values are in good agreement with those obtained from the dynamic simulations. More careful inspection indicates that the experimental values are not continuous when $\omega > 30$ under the condition of $\varphi_i = 60°$. The main reason for this discontinuity is that the adopted servos may lose its performance and fail to track the desired amplitudes in the case of high-frequency, large-amplitude oscillations. But in the dynamic model, these realistic limiting factors are omitted, followed by an increasing trend between the propulsive speed and the frequency. The built dynamic model can thereby be viewed as authoritative under normal conditions.

Next, using the built dynamic model as an evaluation platform, we set out to maximize the forward swimming speed governed by the PSO-based CPG network. With a full consideration of the characteristics of fishlike swimming and the limiting factors of the robotic prototype, the range of CPG parameters is tabulated in Table I. As for the adopted PSO algorithm, the number of particle in the swarm is 20 and the iteration times are 100. The accelerative constants c_1 and c_2 are both 2.0. To avoid the prematurity and diversity reduction of the PSO, five random disturbances are added to the current optimal results. With the optimized CPG parameter set listed

TABLE II
OPTIMIZED PARAMETERS OF THE CPGs

m_1	m_2	m_3	m_4	ω	φ
13.70	19.08	33.50	49.39	29.61	60.0°

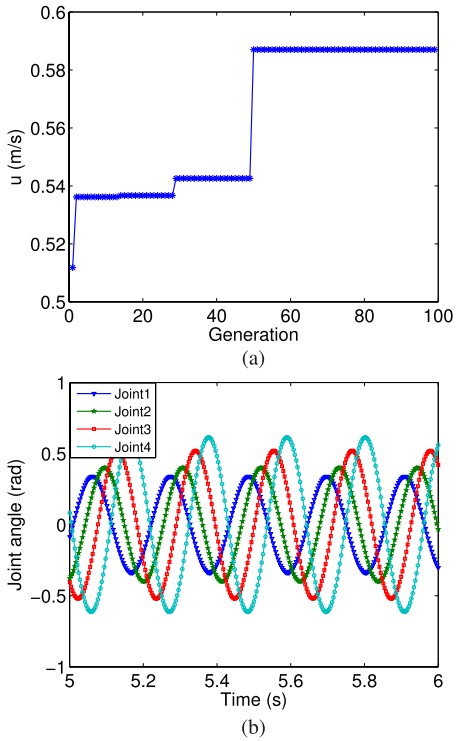

Fig. 4. Simulation results of speed optimization on forward swimming. (a) Obtained maximum speed in simulation. (b) Output signals of the CPG model in simulation.

in Table II, the robotic fish reaches a maximum forward swimming speed of 0.587 m/s. The speed profile and the applied CPG signals are plotted in Fig. 4. Notice that the optimization results show three steps. This is because the global best position represents the maximum speed. In each iteration, the maximum speed will be changed if the new global best position is better than the present one, or else the maximum speed remains the same. Afterward, the optimized parameter set was applied to the robotic prototype. Remarkably, the robot achieved a top speed of 0.57 m/s, corresponding to 1.15 BL/s. A snapshot sequence of forward swimming test is also shown in Fig. 5. We remark that a visual marker which is positioned near the actual mass center of the robot was added to the head during swimming tests, allowing relatively accurate measurement.

In addition, we examined the possibility of backward swimming on the same robotic platform. For the sake of comparison, we first maintained the optimized amplitudes from the forward swimming speed optimization, while directly optimizing the oscillation frequency. In particular, the phase parameter φ was selected as $-75°$ instead of $-60°$ for more smooth and stable backward swimming [30] (Fig. 6). As expected, the robotic fish successfully performed backward swimming with $\varphi = -75°$. Afterward, we tested two different amplitudes (Amp1 and Amp2 via modulating d_i) and phase relations ($-75°$ and $-90°$). As shown in Figs. 7 and 8, a maximum backward swimming speed of 0.25 m/s (corresponding to 0.51 BL/s, less than one half of the maximum forward swimming speed) was achieved at $\omega = 36$, not at $\omega = 40$. This phenomenon may be due to insufficient servo torque output offered at higher frequencies.

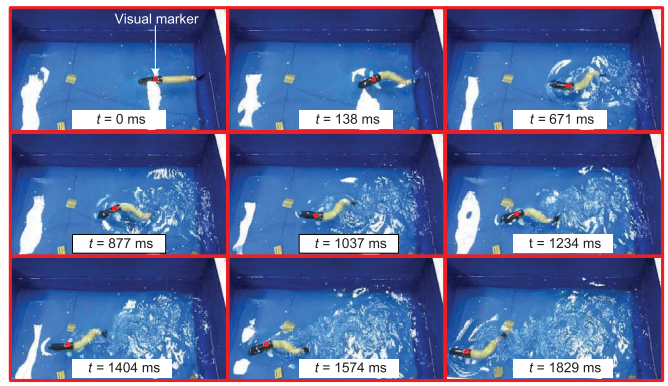

Fig. 5. Snapshot sequence of a forward swimming test.

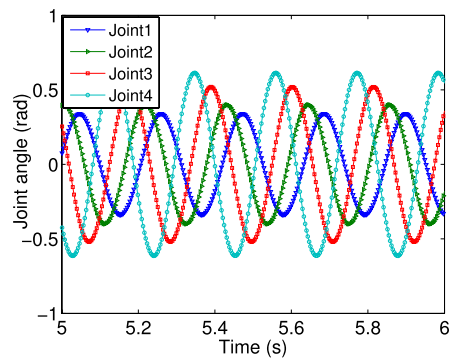

Fig. 6. Output signals of the CPG model for backward swimming with $\varphi = -75°$.

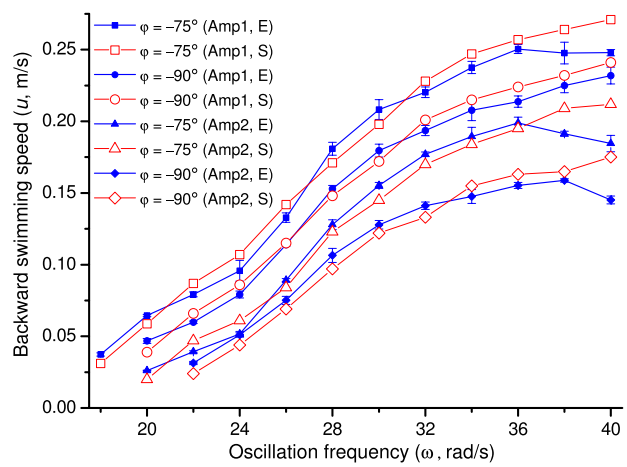

Fig. 7. Comparison of simulated and experimental backward swimming data under different oscillation frequencies, where Amp1 = $\{m_1 = 13.70, m_2 = 19.08, m_3 = 33.50, m_4 = 49.39$, and $d_i = 5.0\}$ and Amp2 = $\{m_1 = 13.70, m_2 = 19.08, m_3 = 33.50, m_4 = 49.39$, and $d_i = 3.0\}$.

B. Discussion

Biological CPG network serves as an effective paradigm for the robotic locomotion, especially for the rhythmic patterns. As for the robotic fish, the quality of the adopted CPG network has a significant effect on its locomotion performance. Therefore, it is extremely essential to optimize the CPG network. Based on the fish body wave method, a lot of studies were done for the optimization of CPG network for the robotic fish [15], [16]. Maybe, it is much more efficient to adopt the direct optimization approach. After all, the robotic fish is distinguished from real fish in structure and function.

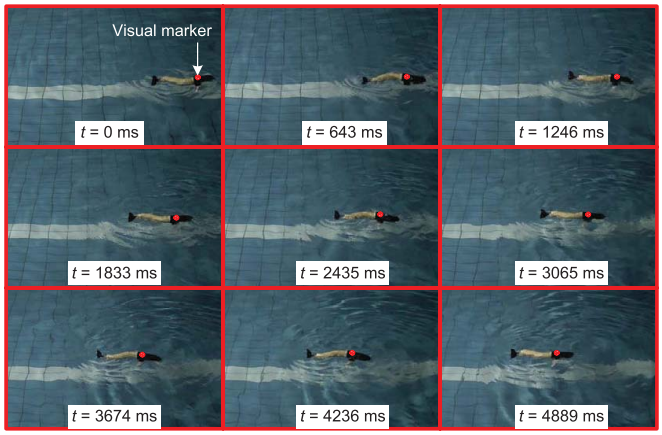

Fig. 8. Snapshot sequence of a backward swimming test.

The parameters obtained from real fish are not necessarily optimal for the robotic fish. As demonstrated above, it is an effective approach for the optimization of the CPG network to adopt the direct performance indicators. Simulation and experimental results verify the presented PSO-based CPG parameter optimization method. In contrast to other similar methods, the optimization procedure removes the need of setting parameters for fish body equations, or designing traveling wave of fishlike swimming. More remarkably, using the achievable maximum propulsive speed as a measure, our robotic fish with optimized CPG parameters peaked 1.15 BL/s, entirely superior to the reported results on miniature robotic fish [21]–[23]. Recently, Clapham and Hu reported that a 0.2-m-long single electric motor actuated and tethered carangiform robotic fish, iSplash-I, can reach 2.8 BL/s in the forward movement [31]. By means of CPG-based swimming control, a similar 0.37-m-long single-motor-two-joint actuated robotic fish achieves an average velocity of 3.07 BL/s when swimming forward, which is higher than that of iSplash-I [32]. In this sense, as a specific neural network, the CPG-based locomotion scheme is promising in achieving high-speed swimming. In addition, based on the same optimized amplitudes, forward and backward swimming motions are compared on the same robotic platform. The robotic fish reached a top backward swimming speed of 0.51 BL/s, less than one half of the maximum forward swimming speed. Even so, this result may be the best backward performance reported in the anguiform/carangiform robotic fish [22], [23].

Concerning the limitation of the applied CPG network optimization, we would like to emphasize that sensory feedback is not incorporated into the control loop at present. Essentially, the CPG network is well suited to coordinate mechanical and neural dynamics or motion of nearby body segments by employing the sensory inputs. Online optimization for the CPG network is also important for improving the robots locomotor skills in dynamic and unstructured environments. With such continuous improvements on online learning and optimization, the adaptability and applicability of the robotic fish will ultimately be expanded.

V. Conclusion

In this brief, we have proposed a direct CPG network optimization method to maximize both forward and backward swimming performance of a self-propelled multijoint robotic fish, with the main emphasis placed on control methods and experimental verification. To guide possible optimization of the CPG network, a relatively accurate dynamic model is developed to numerically evaluate the swimming performance of the robotic fish. Next, the standard PSO with several chaos random disturbances is exploited to further seek the optimal parameters to maximize the average propulsive speed. Simulation and experimental results on the speed optimization are given to show the effectiveness of the employed optimization schemes. In particular, the optimized results highlight the capability of the robotic fish to perform fast forward and backward swimming, affording some valuable insight into the applications of the robotic fish for a specific underwater task.

Acknowledgment

The authors would like to thank the anonymous reviewers for their valuable comments and suggestions on improving this brief.

References

[1] L. Han, Z. Wang, A. Ji, and Z. Dai, "The mechanics and trajectory control in locust jumping," *J. Bionic Eng.*, vol. 10, no. 2, pp. 194–200, 2013.

[2] R. M. Shelton, P. J. M. Thornycroft, and G. V. Lauder, "Undulatory locomotion of flexible foils as biomimetic models for understanding fish propulsion," *J. Experim. Biol.*, vol. 217, no. 12, pp. 2110–2120, 2014.

[3] M. S. Triantafyllou and G. S. Triantafyllou, "An efficient swimming machine," *Sci. Amer.*, vol. 272, no. 3, pp. 40–48, Mar. 1995.

[4] J. Yu, M. Tan, S. Wang, and E. Chen, "Development of a biomimetic robotic fish and its control algorithm," *IEEE Trans. Syst., Man, Cybern. B, Cybern.*, vol. 34, no. 4, pp. 1798–1810, Apr. 2004.

[5] J. Liu and H. Hu, "Mimicry of sharp turning behaviours in a robotic fish," in *Proc. IEEE Int. Conf. Robot. Autom.*, Barcelona, Spain, Apr. 2005, pp. 3318–3323.

[6] J. Liang, T. Wang, and L. Wen, "Development of a two-joint robotic fish for real-world exploration," *J. Field Robot.*, vol. 28, no. 1, pp. 70–79, 2011.

[7] A. J. Ijspeert, "Central pattern generators for locomotion control in animals and robots: A review," *Neural Netw.*, vol. 21, no. 4, pp. 642–653, 2008.

[8] J. Yu, M. Tan, J. Chen, and J. Zhang, "A survey on CPG-inspired control models and system implementation," *IEEE Trans. Neural Netw. Learn. Syst.*, vol. 25, no. 3, pp. 441–456, Mar. 2014.

[9] J. Yu, R. Ding, Q. Yang, M. Tan, and J. Zhang, "Amphibious pattern design of a robotic fish with wheel-propeller-fin mechanisms," *J. Field Robot.*, vol. 30, no. 5, pp. 702–716, 2013.

[10] T. Bliss, T. Iwasaki, and H. Bart-Smith, "Central pattern generator control of a tensegrity swimmer," *IEEE/ASME Trans. Mechatronics*, vol. 18, no. 2, pp. 586–597, Apr. 2013.

[11] A. Crespi, D. Lachat, A. Pasquier, and A. J. Ijspeert, "Controlling swimming and crawling in a fish robot using a central pattern generator," *Auto. Robots*, vol. 25, nos. 1–2, pp. 3–13, 2008.

[12] D. Zhang, D. Hu, L. Shen, and H. Xie, "Design of an artificial bionic neural network to control fish-robot's locomotion," *Neurocomputing*, vol. 71, nos. 4–6, pp. 648–654, 2008.

[13] Z. Wu, J. Yu, Z. Su, and M. Tan, "An improved multimodal robotic fish modelled after *Esox lucíus*," in *Proc. IEEE Int. Conf. Robot. Biomimetics*, Shenzhen, China, Dec. 2013, pp. 516–521.

[14] M. Wang, J. Yu, and M. Tan, "Parameter design for a central pattern generator based locomotion controller," in *Intelligent Robotics and Applications*, vol. 5314. Berlin, Germany: Springer-Verlag, 2008, pp. 352–361.

[15] I.-B. Jeong, C.-S. Park, K.-I. Na, S. Han, and J.-H. Kim, "Particle swarm optimization-based central patter generator for robotic fish locomotion," in *Proc. IEEE Congr. Evol. Comput.*, New Orleans, LA, USA, Jun. 2011, pp. 152–157.

[16] Y. Hu, J. Liang, and T. Wang, "Parameter synthesis of coupled nonlinear oscillators for CPG-based robotic locomotion," *IEEE Trans. Ind. Electron.*, vol. 61, no. 11, pp. 6183–6191, Nov. 2014.

[17] X. Niu, J. Xu, Q. Ren, and Q. Wang, "Locomotion learning for an anguilliform robotic fish using central pattern generator approach," *IEEE Trans. Ind. Electron.*, vol. 6, no. 9, pp. 4780–4787, Sep. 2014.

[18] Z. Wu, J. Yu, and M. Tan, "CPG parameter search for a biomimetic robotic fish based on particle swarm optimization," in *Proc. IEEE Int. Conf. Robot. Biomimetics*, Guangzhou, China, Dec. 2012, pp. 563–568.

[19] J. Yu, M. Wang, Z. Su, M. Tan, and J. Zhang, "Dynamic modeling of a CPG-governed multijoint robotic fish," *Adv. Robot.*, vol. 27, no. 4, pp. 275–285, 2013.

[20] J. Kennedy and R. Eberhart, "Particle swarm optimization," in *Proc. IEEE Int. Conf. Neural Netw.*, Washington, DC, USA, Nov./Dec. 1995, pp. 1942–1948.

[21] C. Wang, G. Xie, L. Wang, and M. Cao, "CPG-based locomotion control of a robotic fish: Using linear oscillators and reducing control parameters via PSO," *Int. J. Innov. Comput. Inf. Control*, vol. 7, no. 7B, pp. 4237–4249, 2011.

[22] X. Niu, J. Xu, Q. Ren, and Q. Wang, "Locomotion generation and motion library design for an anguilliform robotic fish," *J. Bionic Eng.*, vol. 10, no. 3, pp. 251–264, 2013.

[23] C. Zhou, Z. Cao, Z.-G. Hou, S. Wang, and M. Tan, "Backward swimming gaits for a carangiform robotic fish," *Neural Comput. Appl.*, vol. 23, nos. 7–8, pp. 2015–2021, 2013.

[24] M. J. Lighthill, "Note on the swimming of slender fish," *J. Fluid Mech.*, vol. 9, no. 2, pp. 305–317, 1960.

[25] J. E. Colgate and K. M. Lynch, "Mechanics and control of swimming: A review," *IEEE J. Ocean. Eng.*, vol. 29, no. 3, pp. 660–673, Jul. 2004.

[26] J. Buchli and A. J. Ijspeert, "Distributed central pattern generator model for robotics application based on phase sensitivity analysis," in *Biologically Inspired Approaches to Advanced Information Technology* (Lecture Notes in Computer Science), vol. 3141. Berlin, Germany: Springer-Verlag, 2004, pp. 333–349.

[27] Y. Shi and R. Eberhart, "A modified particle swarm optimizer," in *Proc. IEEE Int. Conf. Evol. Comput.*, Washington, DC, USA, May 1998, pp. 69–73.

[28] L. Poli, P. Rocca, L. Manica, and A. Massa, "Handling sideband radiations in time-modulated arrays through particle swarm optimization," *IEEE Trans. Antennas Propag.*, vol. 58, no. 4, pp. 1408–1411, Apr. 2010.

[29] X. Hong, J. Gao, S. Chen, and C. J. Harris, "Particle swarm optimisation assisted classification using elastic net prefiltering," *Neurocomputing*, vol. 122, pp. 210–220, Dec. 2013.

[30] K. D'Août and P. Aerts, "A kinematic comparison of forward and backward swimming in the eel *Anguilla anguilla*," *J. Experim. Biol.*, vol. 202, no. 11, pp. 1511–1521, 1999.

[31] R. J. Clapham and H. Hu, "iSplash-I: High performance swimming motion of a carangiform robotic fish with full-body coordination," in *Proc. IEEE Int. Conf. Robot. Autom.*, Hong Kong, May/Jun. 2014, pp. 322–327.

[32] C. Zhang, J. Yu, and M. Tan, "Swimming performance of a robotic fish in both straight swimming and making a turn," in *Proc. IEEE Int. Conf. Mechatronics Autom.*, Beijing, China, Aug. 2015, pp. 1111–1115.